Identification of the crucial regulatory elements modulating the host respiratory response to SARS-CoV-2 using motif detection, A systems biology approach

Seyed Amir Mirmotalebisohi[a,b], Zahra Molavi[c], Sara Razi[c,d], Marzieh Sameni[a,b], Farshid Karami[e], Mohsen Yazdani[f], Mohammad Mehdi Ranjbar[g], Vahid Niazi[e], Ameneh Jafari[a,c], Amir Jafar Adibi[h], Payman Firouzabadi[i], Hakimeh Zali[c,e*]

[a] Student Research Committee, Department of Biotechnology, School of Advanced Technologies in Medicine, Shahid Beheshti University of Medical Sciences, Tehran, Iran; [b] Cellular and Molecular Biology Research Center, Shahid Beheshti University of Medical Sciences, Tehran, Iran; [c] Proteomics Research Center, Shahid Beheshti University of Medical Science, Tehran, Iran; [d] Department of Biology, Science and Research Branch, Islamic Azad University, Tehran, Iran; [e] Department of Tissue Engineering and Applied Cell Sciences, School of Advanced Technologies in Medicine, Shahid Beheshti University of Medical Sciences, Tehran, Iran ; [f] Institute of Biochemistry and Biophysics, Tehran University, Tehran, Iran; [g] Razi Vaccine and Serum Research Institute, Agricultural Research, Education and Extension Organization, Karaj, Iran; [h] Departments of Orthopedics, School of Medicine, Shahid Beheshti University of Medical Sciences, Tehran, Iran; [i] Department of Biology, Central Tehran Branch, Islamic Azad University, Tehran, Iran

Corresponding author**: Hakimeh Zali. Proteomics Research Center, Shahid Beheshti University of Medical Science, Tehran, Iran. Department of Tissue Engineering and Applied Cell Sciences, School of Advanced Technologies in Medicine, Shahid Beheshti University of Medical Sciences, Tehran, Iran. ***E-mail: hakimehzali@gmail.com, h.zali@sbmu.ac.ir; ***Tel***: +98-21 22439848

Submitted: 2020-01-06; **Accepted:** 2020-03-19; **Published Online**: 2020-04-01; **DOI**: *10.22037/rrr.v5i1.30069*

Introduction: SARS-CoV-2, as a major threat to human health and economy, has brought in uncertain consequences in the early decade of the 21st century. Since no antiviral therapy or effective vaccine against SARS-CoV-2 is currently available, deciphering the possible mechanisms by which the host responds to the virus seems critical, as it may affect the scientific community around the world toward the development of novel therapeutics. Here, we identified the key regulatory molecules modulating the host response to SARS-CoV-2 that affected the transcriptional profiles of respiratory infections in vitro. **Materials and Methods:** We used the data recently published on the effect of SARS-CoV-2 on two lung cell lines. We selected the shared differentially expressed genes (DEGs) between the two cell lines. To find the key regulatory molecules, we used transcription factors-miRNA-gene interaction databases and analyzed the data using the FANMOD software to detect the crucial regulatory motifs. Cytoscape was then applied to construct the network. We used the KEGG pathway and Gene Ontology (GO) enrichment analysis to predict the probable intermediating biochemical pathways and biological processes. **Results:** Our data demonstrated that four triangle-shaped (3edge) feed-forward loop motifs (FFLs) played significant roles, and the integrated FFLs subnetwork was constructed. STAT1, IRF9, IRF7, and PRK12 were the genes shared among them. The most important biological processes relating to the effect of the new virus were linked to response to cytokine, innate immune response, and adaptive immune response. Besides, significantly enriched pathways associated with other different viral infections included the nuclear factor κ-light-chain-enhancer of activated B cells (NF-kappa B) signaling pathway, the nucleotide-binding oligomerization domain-like (NOD-like) receptor signaling pathway, and the Jak-STAT signaling pathway. **Conclusion:** Most of the pathways were related to the cytokines storm that may contribute to different levels of lung injury. These regulatory motifs shed light on the transcriptional signature of the respiratory cells and may be responsible for the development of COVID-19 or can also be used as a potential target for further drug therapies or vaccines.

Keywords: SARS-CoV-2; COVID-19; Motif; Network; Systems biology

Introduction

Acute respiratory distress syndrome (ARDS) and severe lung injury are the results of infection with the current pandemic of COVID-19 that often drives to the decrease of lung function and even death(1). Coronaviruses Disease-2019 (COVID-19) emerges from the third deadly human coronavirus in the past two decades, known as SARS-CoV-2. The death rate of COVID-19 remains to be ascertained (1, 2). SARS-CoV-2 is a type of RNA virus that has the most extended RNA genome among known viruses to date (3, 4). Their genome is enclosed by a lipid bilayer envelope containing spikes and membrane proteins (5). New Corona Viruses (nCoV) bind to their host cell receptors through binding by their spiky protein and release their viral genome into the cell (6). SARS-CoV-2 has been reported to attack the respiratory tract and gastrointestinal tract through Angiotensin Convertase Enzyme 2 (ACE2)(7). ACE2 is considered to be a candidate for drug targeting, while the beneficial effect remains to be proved (8).

Mesenchymal stem cells (MSCs) therapy is one of the possible curative treatments available for COVID-19. Some MSCs are well-known as anti-inflammatory treatments, which also secret paracrine factors, thereby help tissue repair. They have immunomodulatory effects, and since cytokine storming is the main problem of many severe COVID-19 cases, MSCs therapies are under evaluation as a probable resort (9, 10). Some types of MSCs, such as umbilical cord MSC, can also be readily proliferated and home to inflammatory locations in the body (11, 12). Umbilical cord MSCs (UC-MSCs) are considered the best choice for MSC therapies since they are a great source of stem cells and are not immunogenic or tumorigenic. They are also extractable non-invasively (13).

Several clinical trials are currently being conducted in different phases in COVID-19 patients. In one study published on a limited number (seven) of patients, carried out by Dr. Zhao and collaborators, seven patients with COVID-19 pneumonia showed overall extraordinary improvement after 2-4 days of receiving intravenous injection by 1 million MSCs per kilogram in comparison with the control group (10). At the moment, some UC-MSCs and dental pulp stem cells are registered in the Cochrane databank (Registration codes are NCT04288102, NCT04302519, NCT04293692, NCT04269525) (9). A clinical trial is registered by Beijing 302 Hospital that is a multi-center phase 1 trial. They are supposed to recruit 20 COVID-19 patients to evaluate the safety of UC-MSCs therapy for COVID-19 patients with pneumonia. A phase 2 trial is registered to assess the effect of UC-MSCs in treating the new Coronavirus pneumonia by Zhongnan Hospital. Two other clinical trials were registered by Wuhan union hospital and the Puren hospital. Each of them is supposed to recruit 48 patients in two groups receiving 0.5 x 10^6 UC-MSCs /kg intravenous four times every other day. They have postulated that MSCs can help the regeneration of tissues, can lead to apoptotic resistance, and suppress the fibrotic events in tissues (13).

Since most beneficial effects of cell therapy remain to be approved in several next months, to promote the possibility of discovering other treatments for SARS-CoV-2, we need to predict the biological interaction between virus and host. The high morbidity and mortality rate is somewhat a consequence of this interaction (14). So in this study, by bioinformatics analysis of regulatory elements obtained from limited experimental studies and public databases, we tried to predict underlying mechanisms associated with the regulatory network motifs that are probably responsible for the SARS-CoV-2 effect in the respiratory organ.

Transcription Factors (TF) and microRNAs (miRNA), among all gene regulatory layers, have been considered as the most essential gene regulatory elements of biological regulatory networks (15). They usually play roles in different biological processes and the progression of various diseases. TFs are responsible for gene expression at the transcription level, while miRNAs that typically appear in long non-coding 22-nucleotides RNAs play roles at the post-transcriptional level (16).

Among the motifs detected in omics data, feed-forward loops (FFL) were more considered in disease development (17, 18). An FFL contains two regulatory elements that one of which regulates the other to control gene expression. We hypothesized a set of motifs, including FFL, responsible for gene expression in respiratory tissue that finally direct to lung damage. Recently it has been reported a collection of transcription profiles of normal and cancerous lung cells that were exposed to the coronavirus(2). We used this data and extracted the regulatory elements from various public databases to find the statistically significant TF-miRNA-gene motifs related to the effect of SARS-CoV-2 on respiratory cells.

Materials and Methods

Data related to respiratory infection

Data collected from the study published recently by Daniel Blanco-Melo et al. aimed to study respiratory infections at various levels, including in vitro, ex vivo, and in vivo. They compared the transcription responses of seasonal influenza A (IAV) virus, SARS-CoV-2, and human Orthopeneumovirus. The authors applied the primary Normal human bronchial epithelial (NHBE) and the transformed lung alveolar cells (A549) for their in vitro study models. A549 cells were infected with SARS-CoV-2 at a multiplicity of infection (MOI) of 0.2 virus particles per cell for 24 hours, while NHBE cells were treated at an MOI of 2 for 24 h. Total RNA from infected and mock cells was extracted, and RNA-seq libraries were prepared according to the TruSeq RNA Library protocol (Illumina). cDNA libraries were then sequenced using an Illumina NextSeq 500 platform (www.illumina.com) (14). In the present study, we selected genes that were differentially expressed in comparison with mock cells (DEG) and were shared between the two cell lines for further analysis. The shared genes were obtained using the Venn diagram software (http://bioinformatics.psb.ugent.be).

Transcription factors and miRNAs related to the DEGs

TF nodes regulating genes were retrieved from Enrichr (http://amp.pharm.mssm.edu/Enrichr/). Enrichr is a free gene set enrichment analysis web-based tool rendering multiple types of visualization reports of corporate functions of gene lists. It distributes a complete source for curated gene sets and a search engine that incorporates biological science for further biological

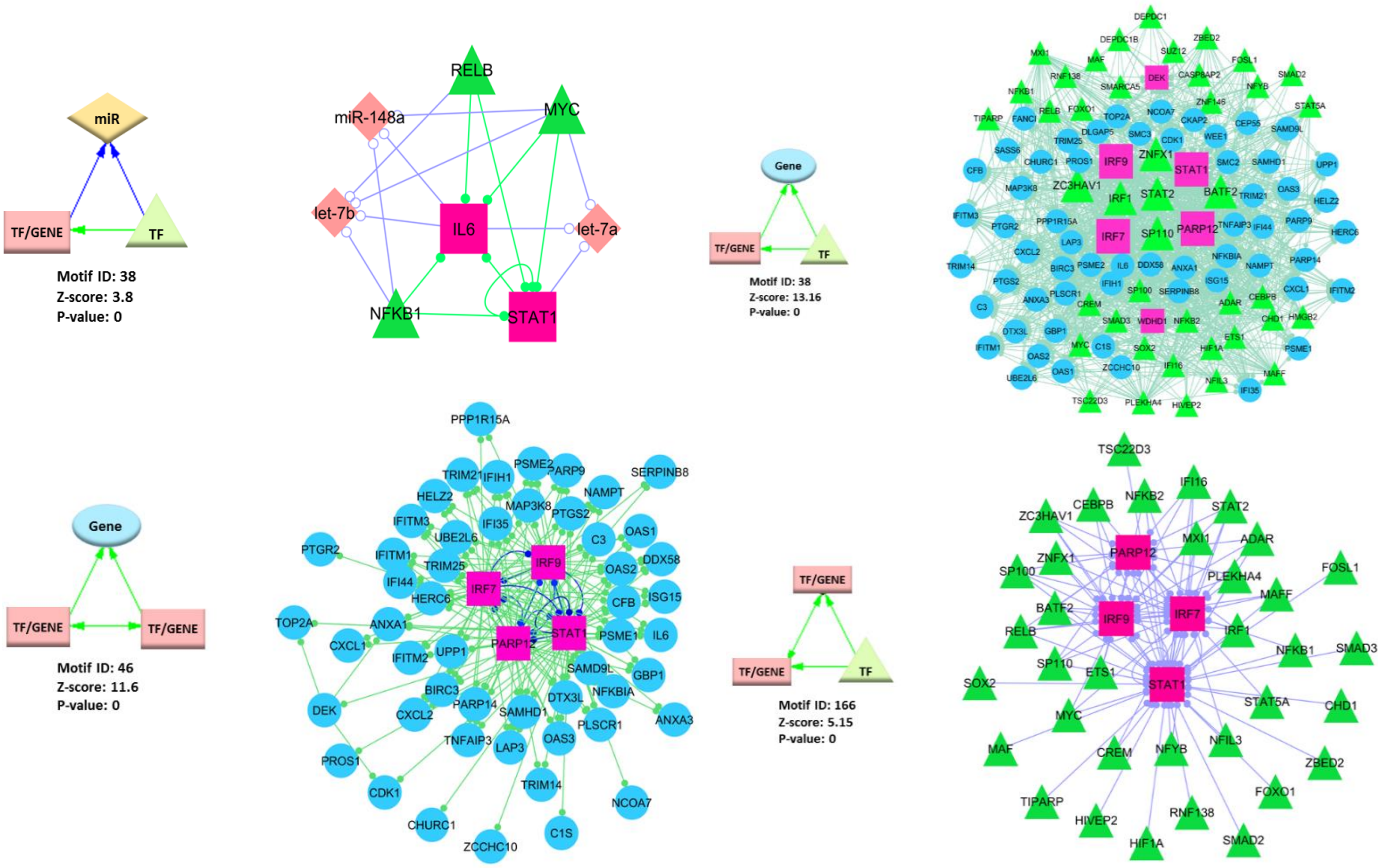

Figure 1. Each section depicts one of the four FFL motifs and its sub-network, comprised of different nodes regulating DEGs in A549 and NHBE cells treated with SARS-CoV-2. Triangle nodes show only TFs, diamond nodes represent miRNAs, ellipse nodes depict only genes, and rectangle nodes depict both TFs and genes (nodes with dual roles). The regulatory nodes modulate the shared DEGs between the A549 and NHBE cell lines. All FFL motifs are represented by their identification motif number in the FANMOD software encyclopedia. *Z*-scores (>2) and *P*-values (<0.05) are reported for each motif. A) The FFL motif contains two types of regulatory elements, including TFs and miRNAs. B, C, and D) The FFLs contain TFs and genes.

explorations (19, 20). We used different regulatory databases, including ARCHS (https://amp.pharm.mssm.edu/archs4/), ChEA (https://www.chea.org/directories), ENCODE (https://www.encodeproject.org/), TRRUST(https://www.grnpedia.org/trrust/) to find the TFs related to the genes.

MiRNAs regulating genes were detected using Enrichr Tool (125 miRNAs by miRTarBase and 32 miRNAs by TargetScan). We also used genetrail2 web tool (https://genetrail2.bioinf.uni-sb.de/), which acts similarly to the Enrichr Tool (219 miRNAs by mirDB and 33 miRNAs by miRWalk).

The third regulatory relationships were the miRNAs regulating TFs, which were extracted using the Enrichr tool (miRTarBase and target Scan databases) to find the existing relations.

TFs regulating miRNAs

For extracting the TFs regulating miRNAs, we used the TransmiR database. TransmiR is an open-source database for transcription factor-microRNA regulations. It identifies the TFs that directly interact with the miRNA precursor genes and control the expression of miRNAs(21).

Motifs detection

To find the transcription factor-microRNA-target gene motif, we applied the algorithm used in our previous work with the same setting details (18). Then we merged the regulatory data obtained from the previous steps and constructed a regulatory network. The four types of regulatory data were put together in an Excel software sheet table and were exported to FANMOD software to find the motif with three nodes (22). FANMOD software is a network motif detection tool. It finds subgraphs

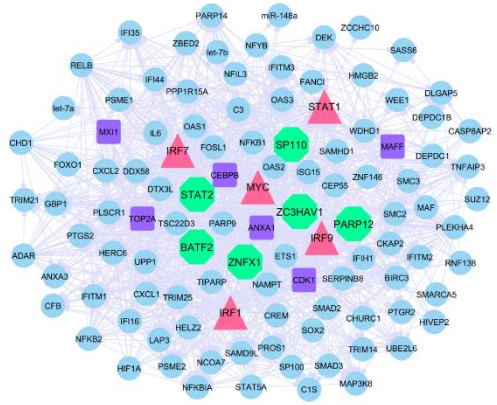

Figure 2. The figure shows the merged miRNA-TF-gene sub-network of the four FFL motifs. Ellipse nodes are the shared DEGs between the A549 and NHBE cells. Rectangle nodes show hubs, octagon nodes depict bottlenecks, and triangle nodes represent both hubs and bottlenecks. The top 10% of nodes with the highest degree (highly connected) were identified as hubs. The top 10% of the nodes with the highest betweenness centrality were considered bottleneck nodes.

that occur significantly in the real network more often than detected in 1000 random networks and determined by Z-score. To detect three-node size motifs, we identified those with Z-score> 2.0 and *P*-value<0.05.

Motif-specific sub-network construction

To construct the gene regulatory network, we used Cytoscape software (version 3.5.1). The sub-networks related to each significantly scored motif (which had both 3nodes and 3edges) were visualized by Cytoscape separately and merged. Nodes having the highest degree ranks in degree ranking were selected as hubs (top 10% of the nodes). The nodes with the highest betweenness centrality (top 10% of the nodes) were nominated as bottlenecks. Both hub and bottleneck nodes were considered as possible crucial nodes.

Gene ontology and Biochemical pathway enrichment analysis

Genes and TFs composing the 3node subnetworks were analyzed using the STRING database (string-db.org). Gene Ontology (GO, www.geneontology.org) and Kyoto Encyclopedia of Genes and Genomes (KEGG, ww.genome.ad.jp/KEGG) enrichment analysis were performed. GO serves as default categorization for biological process, molecular function, and cellular component. It is widely used in bioinformatics and increases the likelihood of identifying the biological process of correlation (BP). KEGG was used to understand the most relevant biochemical pathways related to the genes.

Results

Identification of genes, TFs and miRNAs in respiratory infection by SARS-CoV-2

Based on *P*-value <0.05, 1536 DEGs were identified in A549 and 1136 DEGs in NHBE (Supplementary Table S1). Supplementary Figure S1 represents the Venn diagram of shared DEGs between A549 and NHBE cells that were 134 shared DEGs.

TFs that regulate the genes were obtained by Enrichr tool using its different database subparts including ARCHS4 (104 TFs), ChEA (33 TFs), ENCODE (249 TFs), TRRUST (32 TFs), and Enrichr gene co-occurrence (999 TFs). They were selected based on P-value<0.05. Shared TFs presented in at least two databases were selected. They included 152 TFs. We compared all DEGs in A549 and NHBE cells with those 152 TFs and found six TFs were expressed in both cell lines. As represented in Supplementary Figure S2, we found that 23 of all were only shared with A549 cell line DEGs, and 19 of them were shared only with DEGs of NHBE cells. We selected the combination of the 48 TFs (6+19+23) for further analysis. The genes enrichment for miRNAs based on P-value<0.05, resulted in 125 miRNAs (miRTarBase), 32 miRNAs (TargetScan), 219 miRNAs (miRDB), and 33 miRNAs (miRWalk). Our next selection criterion was the presence of a miRNA in at least two different micro RNA databases. As represented in Supplementary Table S3 and Supplementary Figure S3, we finally obtained 29 miRNAs for the shared DEGs between A549 and NHBE cells treated with SARS-CoV-2.

The next regulatory relationships were the miRNAs regulating TFs. We detected 174 miRNAs for TFs (Supplementary Table S4). The fourth relationship, TFs regulating miRNAs, were retrieved using the TRANSMIR database. We found 55 TFs regulating miRNAs shown in the S5 Supplementary Table.

Motif detection and regulatory network construction

To extract the network regulatory motif containing the transcription factor-microRNA-target genes; the four types of the regulatory data were input into the FANMOD software as an incorporated list (Supplementary Table S6). Thirteen significant 3node size motifs were identified as results shown in Supplementary Figure S4. Then we selected the motif composed of three edges. They included four motifs (FFLs) and were used to construct the new sub-networks. As visualized in Figure 1, we found that three of the four significant motifs contained only genes and TFs. The other motif contains TFs and miRNAs as nodes. Table 1 represents the number of nodes available in each

regulatory relationship and the constructed FFLs. We found miRNAs as the gene or TFs regulator in none of the four FFL motifs. FFL motif NO.38 was detected to contain some TF regulatory elements which control the expression of some miRNAs, including let-7a, let-7b, and miR-148a. Two of these mentioned TFs were STAT1 and IL6 that were also observed as shared DEGs in both cell lines A549 and NHBE. They were reported as regulators of let-7a, let-7b, and miR-148a in TRANSMIR database.

Four composite FFLs combined of different nodes (TFs, miRNAs, and genes) could help us predict mechanisms underlying the effect of SARS-CoV-2 on the host cells. The Motif-specific sub-network resulted from the merging of the four FFLs is represented in Figure 2, and the network analysis results are available in Table 2. Network analysis showed that it consisted of 110 nodes and 1177 edges. The resulted network could not be considered as a scale-free network since it contained a lot of TFs that regulated each other; therefore, the percentage of the nodes with high degrees is more in comparison with the typical scale-free biological networks. The cut-off criterion of the hub and bottleneck nodes selection was considered as being among the top 10% higher degree or betweenness in the network. Based on this cut-off level, crucial nodes were recognized in the network and shown in Table 3. Hub and bottleneck nodes usually seem to play essential roles in cell biology. The shared hub and bottleneck nodes were STAT1, IRF1, IRF7, IRF9, and MYC that are highlighted in the network figure. We also compared the four FFLs to investigate the shared nodes among them. We found four nodes as the shared ones, including STAT1, IRF7, IRF9, and PARP12.

Gene ontology and pathway enrichment analysis

To acquire a deeper insight into the underlying mechanisms, we performed various functional analyses using the STRING database, including gene ontology and KEGG biochemical pathway enrichments. The top ten resulted terms of biological process enrichment are reported in Table.4 (all BPs are available in Supplementary Table S7, P-values<0.05). The significant biological processes included response to cytokine, defense response, response to viruses, and innate immune response. Significant molecular function terms were related to DNA binding and transcription regulatory activity (Table 5 and Supplementary Table S8). Based on the significant cellular component terms, most of the genes were located in the nucleus, cytosol, and intracellular organelle lumen (Table 6 and Supplementary Table S9). Top 10 KEGG pathways are represented in Table No.7, and all of the significant ones are available in Supplementary Table S10. They consist of the NOD-like receptor signaling pathway, Herpes simplex infection, Influenza A, Kaposi's sarcoma-associated herpes infection, the NF-kappa B signaling pathway, Hepatitis C and B, the TNF signaling pathway, and HTLV-I infection.

Discussion

Regulatory motifs with TF and miRNA have been demonstrated to play crucial roles in the pathophysiology of diseases and contribute to mechanisms in different conditions. For instance, Liu, Z *et al.* used FFLs analysis in cystic fibrosis to identify proper drug candidates for repurposing (17). FFL containing interferon I was reported as a cause of pathogenesis in rheumatic disease (23). Several FFLs were also seen in prostate cancer (24), schizophrenia (25), and were considered responsible for protective response into oxidative stress in some disease models (26). In this study, we aimed to define the mechanisms related to the effect of SARS-CoV-2 in respiratory cells in 24h incubation by regulatory motifs analysis. For this purpose, FFLs were detected from shared DEGs of the two respiratory cell lines, A549 and NHBE treated for 24h with SARS-CoV-2. Then we integrated the four FFLs and enriched them for gene ontology and KEGG pathways. The primary biological processes were linked to negative and positive innate immune responses and involved more than 35 genes overexpressed or suppressed in the presence of the virus. Some of the top 10 biological processes were related to the cytokine response. These confirm the findings identifying the cytokine storm as the first response in defense against the virus. In the COVID-19 severe cases, high-levels of some inflammatory cytokine proteins were detected, including IL-2, IL-7, IL-10, G-CSF, IP-10, MCP-1, MIP-1A, and TNFα. In ICU patients, higher plasma levels of many innate cytokines were detected, including IP-10, MCP-1, MIP-1A, and TNFα(27).

A549 and NHBE cells under treatment for 24h with SARS-CoV-2 also run the signaling pathways that lead to an effective innate immune response against the viral infection and lead to control viral replication and induce an effective adaptive immune response(28). We found the FFLs contained genes relating to the interferon (IFN) type I pathway, while IFN-I was not expressed in the cell lines. It also seems that the host cell defenses against SARS-CoV-2 through the antiviral mechanisms are seen against other viral diseases. The pieces of evidence for these responses are the KEGG pathways that are enriched for several viral illnesses, including Herpes simplex, Influenza A, Hepatitis C, Hepatitis B, and HTLV-I infection. A previous study has reported that the cytokine storm and the lymphopenia in COVID-19 are in line with SARS and MERS, and they can initiate viral sepsis and inflammation.

Table 1. Summary of the four types of regulatory relationships and the four detected FFLs

Relationship	Source and Target	Count	Genes (n)	TFs (n)	miRNAs (n)
Four regulatory relationships	miRNA → gene	193	82	---	29
	TF → gene	1403	125	48	---
	miRNA → TF	555	---	44	174
	TF → miRNA	77	---	52	15
Four FFLs	miRNA/TF FFLs (ID: 38)	18	2	4	3
	TF FFLs (ID: 38)	1167	70	54	---
	TF FFLs (ID: 46)	184	60	8	---
	TF FFLs (ID: 166)	98	4	43	---

Table 2. Network analysis results containing different parameters related to the composite FFLs. Composite FFLs subnetwork contains all regulatory elements of the four FFLs

Parameters	Values
Number of nodes	110
Number of edges	1177
Network density	0.195
Network heterogeneity	0.687
Number of self-loops	1
Network diameter	3
Network centralization	0.624
Average path length	1.955
Average number of neighbors	21.273

Table 3. The top 10% of nodes were selected as hubs and bottlenecks in the regulatory network

Gene name	Degree	Gene name	Betweenness centrality
STAT1	93	STAT1	0.237504
IRF7	67	IRF1	0.057497
IRF9	63	MYC	0.046122
PARP12	57	IRF7	0.036545
IRF1	52	TOP2A	0.034378
BATF2	45	MXI1	0.03205
STAT2	44	ANXA1	0.029235
ZNFX1	44	CEBPB	0.027196
MYC	42	MAFF	0.025036
ZC3HAV1	42	CDK1	0.024981
SP110	42	IRF9	0.02104

Table 4. The genes enrichment analysis for biological process (GO-BP). Top 10 terms of Biological Processes were selected after being sorted by significant *P*-values<0.05

No	term (Biological Process)	false discovery rate	matching proteins in the network
1	response to cytokine	2.79E-25	ADAR,ANXA1,BIRC3,CEBPB,CXCL1,CXCL2,ETS1,FOSL1,FOXO1,GBP1,HIF1A,IFI35,IFITM1,IFITM2,IFITM3,IL6,IRF1,IRF7,IRF9,ISG15,…
2	defense response	1.24E-23	ADAR,ANXA1,ANXA3,BATF2,C1S,C3,CEBPB,CFB,CXCL1,CXCL2,DDX58,DTX3L,FOSL1,GBP1,HIF1A,HMGB2,IFI16,IFI35,IFIH1,IFITM1…
3	response to other organism	1.24E-23	ADAR,ANXA3,BATF2,C3,CEBPB,CXCL1,CXCL2,DDX58,DTX3L,FOSL1,GBP1,HERC6,HMGB2,IFI16,IFI44,IFIH1,IFITM1,IFITM2,IFITM3,…
4	defense response to virus	7.77E-23	ADAR,DDX58,DTX3L,GBP1,IFI16,IFIH1,IFITM1,IFITM2,IFITM3,IL6,IRF1,IRF7,IRF9,ISG15,OAS1,OAS2,OAS3,PARP9,PLSCR1,SAMHD1,…
5	cellular response to cytokine stimulus	4.11E-22	ADAR,ANXA1,BIRC3,CEBPB,CXCL1,CXCL2,FOXO1,GBP1,HIF1A,IFI35,IFITM1,IFITM2,IFITM3,IL6,IRF1,IRF7,IRF9,ISG15,MAP3K8,MYC,…
6	response to stress	8.68E-22	ADAR,ANXA1,ANXA3,BATF2,C1S,C3,CDK1,CEBPB,CFB,CXCL1,CXCL2,DDX58,DTX3L,ETS1,FANCI,FOSL1,FOXO1,GBP1,HIF1A,HMGB2,..
7	response to virus	8.68E-22	ADAR,DDX58,DTX3L,FOSL1,GBP1,IFI16,IFI44,IFIH1,IFITM1,IFITM2,IFITM3,IL6,IRF1,IRF7,IRF9,ISG15,OAS1,OAS2,OAS3,PARP9,..
8	innate immune response	8.68E-22	ADAR,ANXA1,C1S,C3,CFB,DDX58,DTX3L,GBP1,HMGB2,IFI16,IFI35,IFIH1,IFITM1,IFITM2,IFITM3,IRF1,IRF7,IRF9,ISG15,NFKB1,NFKB2,..
9	cytokine-mediated signaling pathway	3.20E-21	ADAR,ANXA1,BIRC3,CXCL1,CXCL2,FOXO1,GBP1,HIF1A,IFI35,IFITM1,IFITM2,IFITM3,IL6,IRF1,IRF7,IRF9,ISG15,MAP3K8,MYC,NFKB1,..
10	response to cytokine	2.79E-25	ADAR,ANXA1,BIRC3,CEBPB,CXCL1,CXCL2,ETS1,FOSL1,FOXO1,GBP1,HIF1A,IFI35,IFITM1,IFITM2,IFITM3,IL6,IRF1,IRF7,IRF9,ISG15,..

Table 5. Top 10 molecular function terms with significant *P*-value<0.05

No	Term (Molecular Function)	False discovery rate	Matching proteins in the network
1	DNA binding	3.82E-16	ADAR,ANXA1,BATF2,CASP8AP2,CEBPB,CHD1,CREM,DDX58,DEK,ETS1,FANCI,FOSL1,FOXO1,HELZ2,HIF1A,HIVEP2,HMGB2,IFI16,…
2	nucleic acid binding	1.98E-14	ADAR,ANXA1,BATF2,CASP8AP2,CEBPB,CHD1,CREM,DDX58,DEK,ETS1,FANCI,FOSL1,FOXO1,HELZ2,HIF1A,HIVEP2,HMGB2,IFI16,…
3	transcription regulator activity	1.40E-12	BATF2,CASP8AP2,CEBPB,CREM,ETS1,FOSL1,FOXO1,HELZ2,HIF1A,HIVEP2,HMGB2,IFI16,IRF1,IRF7,IRF9,MAF,MAFF,MXI1,MYC,…
4	DNA-binding transcription factor activity	4.08E-12	BATF2,CEBPB,CREM,ETS1,FOSL1,FOXO1,HIF1A,HIVEP2,HMGB2,IFI16,IRF1,IRF7,IRF9,MAF,MAFF,MXI1,MYC,NFIL3,NFKB1,NFKB2,…
5	DNA-binding transcription factor activity, RNA polymerase II-specific	1.23E-11	BATF2,CEBPB,CREM,ETS1,FOSL1,FOXO1,HIF1A,HIVEP2,IFI16,IRF1,IRF7,IRF9,MAF,MAFF,MXI1,MYC,NFIL3,NFKB1,NFKB2,NFYB,…
6	heterocyclic compound binding	9.39E-11	ADAR,ANXA1,BATF2,CASP8AP2,CDK1,CEBPB,CHD1,CREM,DDX58,DEK,ETS1,FANCI,FOSL1,FOXO1,GBP1,HELZ2,HIF1A,HIVEP2,…
7	organic cyclic compound binding	1.61E-10	ADAR,ANXA1,BATF2,CASP8AP2,CDK1,CEBPB,CHD1,CREM,DDX58,DEK,ETS1,FANCI,FOSL1,FOXO1,GBP1,HELZ2,HIF1A,HIVEP2,..
8	transcription regulatory region DNA binding	6.36E-09	CEBPB,CREM,ETS1,FOSL1,HIF1A,HIVEP2,HMGB2,IFI16,IRF1,IRF7,IRF9,MYC,NFIL3,NFKB1,NFKB2,NFYB,RELB,SMAD2,SMAD3,SOX2,…
9	sequence-specific DNA binding	1.52E-08	CEBPB,CREM,ETS1,FOSL1,FOXO1,HIF1A,HIVEP2,HMGB2,IFI16,IRF1,IRF7,IRF9,MAF,MAFF,MYC,NFIL3,NFKB1,NFKB2,NFYB,RELB,…
10	transcription regulatory region sequence-specific DNA binding	6.82E-08	CEBPB,CREM,ETS1,FOSL1,HIF1A,HMGB2,IFI16,IRF1,IRF7,IRF9,MYC,NFIL3,NFKB1,NFKB2,RELB,SMAD2,SMAD3,SOX2,STAT1,SUZ12

Table 6. Top 10 cellular component terms with significant *P*-value<0.05

No	Cellular component	False discovery rate	Matching proteins in the network
1	nucleus	3.60E-12	ADAR,ANXA1,BATF2,BIRC3,CASP8AP2,CDK1,CEBPB,CHD1,CREM,DEK,DEPDC1,DLGAP5,DTX3L,ETS1,FANCI,FOSL1,FOXO1,HELZ2,…
2	nucleoplasm	3.60E-12	ADAR,ANXA1,BIRC3,CASP8AP2,CDK1,CEBPB,CHD1,DEK,DTX3L,ETS1,FANCI,FOSL1,FOXO1,HELZ2,HIF1A,HIVEP2,HMGB2,IFI16,…
3	nuclear lumen	1.11E-11	ADAR,ANXA1,BIRC3,CASP8AP2,CDK1,CEBPB,CHD1,DEK,DTX3L,ETS1,FANCI,FOSL1,FOXO1,HELZ2,HIF1A,HIVEP2,HMGB2,IFI16,IRF1,..
4	intracellular organelle lumen	3.93E-10	ADAR,ANXA1,BIRC3,C3,CASP8AP2,CDK1,CEBPB,CHD1,CXCL1,DEK,DTX3L,ETS1,FANCI,FOSL1,FOXO1,HELZ2,HIF1A,HIVEP2,HMGB2,..
5	cytosol	2.63E-08	ANXA1,ANXA3,BIRC3,CDK1,CKAP2,DDX58,DEPDC1B,DLGAP5,DTX3L,FANCI,FOSL1,FOXO1,GBP1,HERC6,HIF1A,IFI16,IFI35,IFIH1,..
6	intracellular membrane-bounded organelle	4.01E-07	ADAR,ANXA1,BATF2,BIRC3,C3,CASP8AP2,CDK1,CEBPB,CHD1,CREM,DEK,DEPDC1,DLGAP5,DTX3L,ETS1,FANCI,FOSL1,FOXO1,GBP1,..
7	intracellular organelle	4.51E-07	ADAR,ANXA1,ANXA3,BATF2,BIRC3,C3,CASP8AP2,CDK1,CEBPB,CEP55,CHD1,CKAP2,CREM,CXCL1,DDX58,DEK,DEPDC1,DLGAP5,…
8	membrane-bounded organelle	1.25E-06	ADAR,ANXA1,ANXA3,BATF2,BIRC3,C3,CASP8AP2,CDK1,CEBPB,CHD1,CREM,CXCL1,DEK,DEPDC1,DLGAP5,DTX3L,ETS1,FANCI,…
9	intracellular part	1.60E-06	ADAR,ANXA1,ANXA3,BATF2,BIRC3,C3,CASP8AP2,CDK1,CEBPB,CEP55,CHD1,CKAP2,CREM,CXCL1,DDX58,DEK,DEPDC1,DEPDC1B,…
10	I-kappaB/NF-kappaB complex	5.36E-06	NFKB1,NFKB2,NFKBIA,RELB

Table 7. Top 10 KEGG biochemical pathways were selected with a significant *P*-value<0.05.

No	Term (KEGG pathway)	False discovery rate	Matching proteins in the network
1	NOD-like receptor signaling pathway	2.08E-14	BIRC3,CXCL1,CXCL2,GBP1,IFI16,IL6,IRF7,IRF9,NAMPT,NFKB1,NFKBIA,OAS1,OAS2,OAS3,
2	Measles	1.91E-13	ADAR,DDX58,IFIH1,IL6,IRF7,IRF9,NFKB1,NFKBIA,OAS1,OAS2,OAS3,STAT1,STAT2,STAT5A,…
3	Herpes simplex infection	8.39E-12	C3,CDK1,DDX58,IFIH1,IL6,IRF7,IRF9,NFKB1,NFKBIA,OAS1,OAS2,OAS3,SP100,STAT1,STAT2
4	Influenza A	3.94E-11	ADAR,DDX58,IFIH1,IL6,IRF7,IRF9,NFKB1,NFKBIA,OAS1,OAS2,OAS3,STAT1,STAT2,TRIM25
5	Kaposi's sarcoma-associated herpesvirus infection	1.38E-09	C3,CXCL1,CXCL2,HIF1A,IL6,IRF7,IRF9,MYC,NFKB1,NFKBIA,PTGS2,STAT1,STAT2
6	NF-kappa B signaling pathway	5.14E-09	BIRC3,CXCL2,DDX58,NFKB1,NFKB2,NFKBIA,PTGS2,RELB,TNFAIP3,TRIM25
7	Hepatitis C	6.20E-09	DDX58,IRF1,IRF7,IRF9,NFKB1,NFKBIA,OAS1,OAS2,OAS3,STAT1,STAT2
8	Hepatitis B	1.21E-08	DDX58,IFIH1,IL6,IRF7,MYC,NFKB1,NFKBIA,SMAD3,STAT1,STAT2,STAT5A
9	TNF signaling pathway	1.32E-08	BIRC3,CEBPB,CXCL1,CXCL2,IL6,MAP3K8,NFKB1,NFKBIA,PTGS2,TNFAIP3
10	HTLV-I infection	2.59E-08	CREM,ETS1,FOSL1,IL6,MYC,NFKB1,NFKB2,NFKBIA,NFYB,RELB,SMAD2,SMAD3,STAT5A

They can also induce lung injury, which may lead to other complications, including pneumonitis, acute respiratory distress syndrome (ARDS), respiratory failure, shock, organ failure, and potential death (28).

The adaptive immune response containing genes, including ANXA1, C1S, C3, IL6, IRF7, NFKB2, and RELB was also observed, as an enrichment result of the treatment with SARS-CoV-2 after 24 hours. Besides, some signaling pathways activated through the genes included the following: 1-cytokine- mediated signaling pathway, 2-type I interferon signaling pathway, 3-interferon-gamma-mediated signaling pathway, 4-NF-kappaB signaling, 5-MDA-5 signaling pathway, 6-regulation of MyD88-dependent toll-like receptor signaling pathway, 7-regulation of the toll-like receptor signaling pathway, 8-receptor signaling pathway via JAK-STAT, 9-interleukin-1-mediated signaling pathway, 10-interleukin-6-mediated signaling pathway, 11-regulation of extrinsic apoptotic signaling pathway via death domain receptors, 12-retinoic acid receptor signaling pathway, and 13-tumor necrosis factor-mediated signaling pathway. Most of these pathways contribute to the inflammation response that recently has been confirmed by the evidence obtained from patient samples (29, 30).

Interestingly, STAT1, IRF7, IRF9, and PARP12 were found to be the shared genes among all the four detected FFLs. STAT1, as a regulatory element of the JAK-STAT pathway, was up-regulated in both cell lines. The complex of STAT1/2 and IRF9 initiate the transcription of IFN-stimulated genes (ISGs)(2). All these genes usually are up-regulated in response to type I IFN; however, in our study, the interferon I pathway was up-regulated without the effect of type I IFN. A successful outcome of this response leads to overcome viral replication and distribution at the early stage. Transcription factors IRF3 and IRF7 play essential roles in the host response to virus infection by regulating the expression of the IFN-I, IFN-β, and IFN-α genes (31).

M protein of SARS-CoV has been shown to inhibit the production of type I IFN by inhibiting activation of the IRF3/IRF7 transcription factor (32). SARS-CoV-2 also might apply this mechanism to inhibit the expression of IFNs.

Polymerases Poly ADP-Ribose (PARPs), specifically PARP12 and PARP14, are needed to inhibit the reproduction of new corona (CoVs) with mutated macrodomains. Previous studies have reported that CoVs are not able to cause disease in the absence of ADP-ribosylhydrolase. This decrease is accompanied by a decrement in viral load and a change in pro-inflammatory cytokines within the body (33, 34). PARPs played two roles, including antiviral and immunomodulatory (35). The pan-PARP inhibitors reduced IFN and increased the reproduction of mouse hepatitis virus (MHV) lacking ADP-ribosylhydrolase activity; however, they did not have an impact on the wild-type. PARPS antiviral activity depended on their ADP-ribosyltransferase, as these inhibitors target their catalytic site (36).

PARP12, which its sequence has high similarity to PARP13 (ZAP), inhibits viral and cellular protein translation. It also inhibits virus reproduction by some mechanisms, including ADP-ribosylation dependent and independent. The PARP12 gene was reported to be activated during the Venezuelan equine encephalitis virus (VEEV) clearance and attracted our attention. The corresponding protein had a powerful inhibitory impression on the increase of the wild-type and mutant VEEV in vertebrate cells; moreover, the longPARP12 isoform (PARP12L) played an inhibitory role in the reproduction of different alphaviruses and other RNA viruses. It seems it has various antiviral functions due to its inhibitory impact on diverse cellular processes involved in virus reproduction (37).

These four TF-genes, including STAT1, IRF7, IRF9, and PARP12, locating in the center of our FFL network and regulating each other, might be responsible for host defense by amplification of cytokine expression at early 24h. Highly interactions between these TFs imply this fact that immune cells producing inflammatory cytokines might form a positive feedback cycle. Clinical outcome of cytokine storm is probably observed in mild COVID-19 patients shifted to severe phase(38).

Conclusion

FFL-subnetworks of differentially expressed genes in respiratory cells treated with SARS-CoV-2 revealed the biological processes and pathways that enable more immune responses, including cytokine storm, cellular defense, several inflammatory pathways, humoral immune response, innate, and adaptive immune response. The four TF-genes that activated each other were the interesting results obtained from motif analysis that could shed light on the mechanisms behind their up-regulation in host cells. With the limited accessible biological details of respiratory cells response in vivo, this study fills the knowledge gap within in vitro studies. Besides, with the limited available research, we had to analyze all DEGs without separating up-regulated from down-regulated data. In sum, this bioinformatics research might help to understand the regulation behinds the effect of SARS-CoV-2 on respiratory cells that could impact the future designing studies of a prophylactic and therapeutic vaccine.

Acknowledgments

The authors thank the Proteomics Research Center of Shahid Beheshti University of Medical Sciences for their financial support to conduct this survey (NO.22784).

Supplementary Material is available at RRR online

Conflict of Interest: 'None declared'.

References

1. Wu F, Zhao S, Yu B, Chen Y-M, Wang W, Song Z-G, et al. A new coronavirus associated with human respiratory disease in China. Nature. 2020;579(7798):265-9.
2. de Wit E, van Doremalen N, Falzarano D, Munster VJ. SARS and MERS: recent insights into emerging coronaviruses. Nature Reviews Microbiology. 2016;14(8):523.
3. Ziebuhr J. The coronavirus replicase. Coronavirus replication and reverse genetics: Springer; 2005. p. 57-94.
4. Anand K, Ziebuhr J, Wadhwani P, Mesters JR, Hilgenfeld R. Coronavirus main proteinase (3CLpro) structure: basis for design of anti-SARS drugs. Science. 2003;300(5626):1763-7.
5. de Haan CA, Smeets M, Vernooij F, Vennema H, Rottier P. Mapping of the coronavirus membrane protein domains involved in interaction with the spike protein. Journal of virology. 1999;73(9):7441-52.
6. Weiss SR, Navas-Martin S. Coronavirus pathogenesis and the emerging pathogen severe acute respiratory syndrome coronavirus. Microbiol Mol Biol Rev. 2005;69(4):635-64.
7. Gu J, Han B, Wang J. COVID-19: gastrointestinal manifestations and potential fecal–oral transmission. Gastroenterology. 2020.
8. Patel AB, Verma A. COVID-19 and angiotensin-converting enzyme inhibitors and angiotensin receptor blockers: what is the evidence? Jama. 2020.
9. Tu Y-F, Chien C-S, Yarmishyn AA, Lin Y-Y, Luo Y-H, Lin Y-T, et al. A Review of SARS-CoV-2 and the Ongoing Clinical Trials. International journal of molecular sciences. 2020;21(7):2657.
10. Shetty AK. Mesenchymal stem cell infusion shows promise for combating Coronavirus (COVID-19)-induced pneumonia. Aging and disease. 2020;11(2):462.
11. Regmi S, Pathak S, Kim JO, Yong CS, Jeong J-H. Mesenchymal stem cell therapy for the treatment of inflammatory diseases: challenges, opportunities, and future perspectives. European journal of cell biology. 2019.
12. Cell Therapy Using Umbilical Cord-derived Mesenchymal Stromal Cells in SARS-CoV-2-related ARDS (STROMA-CoV2). Randomized: Assistance Publique - Hôpitaux de Paris; 2020.
13. Orleans L, is Vice H, Manchikanti L. Expanded umbilical cord mesenchymal stem cells (UC-MSCs) as a therapeutic strategy in managing critically ill COVID-19 patients: The case for compassionate use. Pain Physician. 2020;23:E71-E83.
14. Blanco-Melo D, Nilsson-Payant B, Liu W-C, Moeller R, Panis M, Sachs D, et al. SARS-CoV-2 launches a unique transcriptional signature from in vitro, ex vivo, and in vivo systems. bioRxiv. 2020.
15. Chen K, Rajewsky N. The evolution of gene regulation by transcription factors and microRNAs. Nature Reviews Genetics. 2007;8(2):93-103.
16. Qin S, Ma F, Chen L. Gene regulatory networks by transcription factors and microRNAs in breast cancer. Bioinformatics. 2015;31(1):76-83.
17. Liu Z, Borlak J, Tong W. Deciphering miRNA transcription factor feed-forward loops to identify drug repurposing candidates for cystic fibrosis. Genome medicine. 2014;6(12):94.
18. Farahani M, Rezaei–Tavirani M, Zali H, Arefi Oskouie A, Omidi M, Lashay A. Deciphering the transcription factor-microRNA-target gene regulatory network associated with graphene oxide cytotoxicity. Nanotoxicology. 2018;12(9):1014-26.
19. Chen EY, Tan CM, Kou Y, Duan Q, Wang Z, Meirelles GV, et al. Enrichr: interactive and collaborative HTML5 gene list enrichment analysis tool. BMC bioinformatics. 2013;14(1):128.
20. Kuleshov MV, Jones MR, Rouillard AD, Fernandez NF, Duan Q, Wang Z, et al. Enrichr: a comprehensive gene set enrichment analysis web server 2016 update. Nucleic acids research. 2016;44(W1):W90-W7.
21. Tong Z, Cui Q, Wang J, Zhou Y. TransmiR v2. 0: an updated transcription factor-microRNA regulation database. Nucleic acids research. 2019;47(D1):D253-D8.
22. Wernicke S, Rasche F. FANMOD: a tool for fast network motif detection. Bioinformatics. 2006;22(9):1152-3.
23. Hall JC, Rosen A. Type I interferons: crucial participants in disease amplification in autoimmunity. Nature Reviews Rheumatology. 2010;6(1):40.
24. Afshar AS, Xu J, Goutsias J. Integrative identification of deregulated miRNA/TF-mediated gene regulatory loops and networks in prostate cancer. PloS one. 2014;9(6).
25. Guo A-Y, Sun J, Jia P, Zhao Z. A novel microRNA and transcription factor mediated regulatory network in schizophrenia. BMC systems biology. 2010;4(1):10.
26. Taylor RC, Acquaah-Mensah G, Singhal M, Malhotra D, Biswal S. Network inference algorithms elucidate Nrf2 regulation of mouse lung oxidative stress. PLoS computational biology. 2008;4(8).
27. Huang C, Wang Y, Li X, Ren L, Zhao J, Hu Y, et al. Clinical features of patients infected with 2019 novel coronavirus in Wuhan, China. The Lancet. 2020;395(10223):497-506.
28. Prompetchara E, Ketloy C, Palaga T. Immune responses in COVID-19 and potential vaccines: Lessons learned from SARS and MERS epidemic. Asian Pac J Allergy Immunol. 2020;38(1):1-9.
29. Zhang W, Zhao Y, Zhang F, Wang Q, Li T, Liu Z, et al. The use of anti-inflammatory drugs in the treatment of people with severe

coronavirus disease 2019 (COVID-19): The experience of clinical immunologists from China. Clinical Immunology. 2020:108393.
30. Martinez MA. Compounds with therapeutic potential against novel respiratory 2019 coronavirus. Antimicrobial Agents and Chemotherapy. 2020.
31. Sato M, Suemori H, Hata N, Asagiri M, Ogasawara K, Nakao K, et al. Distinct and essential roles of transcription factors IRF-3 and IRF-7 in response to viruses for IFN-α/β gene induction. Immunity. 2000;13(4):539-48.
32. Siu K-L, Kok K-H, Ng M-HJ, Poon VK, Yuen K-Y, Zheng B-J, et al. Severe acute respiratory syndrome coronavirus M protein inhibits type I interferon production by impeding the formation of TRAF3· TANK· TBK1/IKKε complex. Journal of Biological Chemistry. 2009;284(24):16202-9.
33. Fehr AR, Athmer J, Channappanavar R, Phillips JM, Meyerholz DK, Perlman S. The nsp3 macrodomain promotes virulence in mice with coronavirus-induced encephalitis. Journal of virology. 2015;89(3):1523-36.
34. Eriksson KK, Cervantes-Barragán L, Ludewig B, Thiel V. Mouse hepatitis virus liver pathology is dependent on ADP-ribose-1 ″-phosphatase, a viral function conserved in the alpha-like supergroup. Journal of virology. 2008;82(24):12325-34.
35. Kuny CV, Sullivan CS. Virus–host interactions and the ARTD/PARP family of enzymes. PLoS pathogens. 2016;12(3).
36. Grunewald ME, Chen Y, Kuny C, Maejima T, Lease R, Ferraris D, et al. The coronavirus macrodomain is required to prevent PARP-mediated inhibition of virus replication and enhancement of IFN expression. PLoS pathogens. 2019;15(5).
37. Atasheva S, Frolova EI, Frolov I. Interferon-stimulated poly (ADP-Ribose) polymerases are potent inhibitors of cellular translation and virus replication. Journal of virology. 2014;88(4):2116-30.
38. Yang Y, Ye F, Zhu N, Wang W, Deng Y, Zhao Z, et al. Middle East respiratory syndrome coronavirus ORF4b protein inhibits type I interferon production through both cytoplasmic and nuclear targets. Scientific reports. 2015;5:17554.

Please cite this paper as: Mirmotalebisohi SA, Molavi Z, Razi S, Sameni M, Karami F, Yazdani M, Ranjbar MM, Niazi V, Jafari A, Adibi AJ, Firouzabadi P, Zali H. Identification of the crucial regulatory elements modulating the host respiratory response to SARS-CoV-2 using motif detection, A systems biology approach. Regen Reconstr Restor. 2020;5(1): e4. Doi: 10.22037/rrr.v5i1.30069.

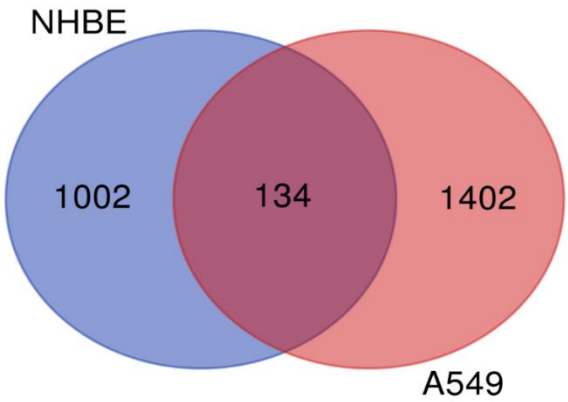

Supplementary Figure S1. Shared DEGs between A549 and NHBE cell lines after treatment with SARSCoV2. Data obtained from the RNA-seq analysis study carried out by Daniel Blanco-Melo *et al.*

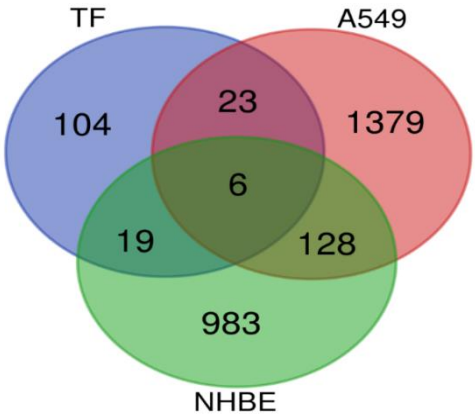

Supplementary Figure S2. TFs from public databases regulating the shared genes between the two cell lines, A549 and NHBE treated with SARS-CoV-2. Out of them, six of the transcription factors are regulating DEGs in both cell lines while 19 TFs regulate DEGs in the NHBE cell line, and 23 TFs regulate DEGs of the A549 cell line

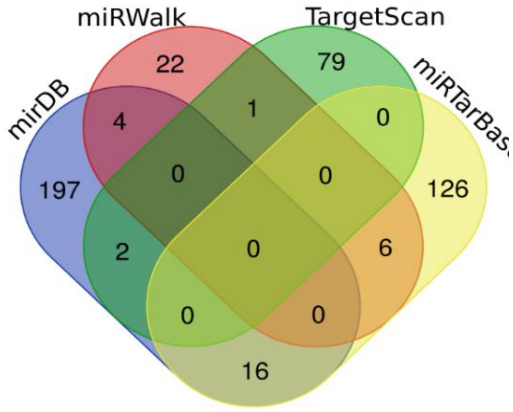

Supplementary Figure S3. miRNAs extracted from public databases regulating the shared DEGs between the two cell lines, A549 and NHBE treated with SARS-CoV-2. There was no shared miRNA among all the databases, so miRNAs shared between at least two databases were detected

ID	Adj	Frequency [Original]	Mean-Freq [Random]	Standard-Dev [Random]	Z-Score	p-Value
36	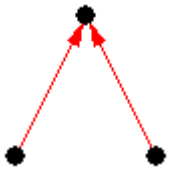	9.158%	8.9666%	0.00014444	13.251	0
12	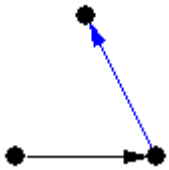	0.0132%	0.012924%	2.082e-007	13.251	0
36	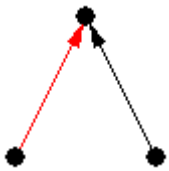	0.070401%	0.068929%	1.1104e-006	13.251	0
6	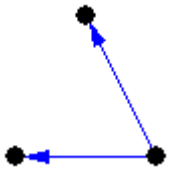	0.073334%	0.071802%	1.1566e-006	13.251	0
12	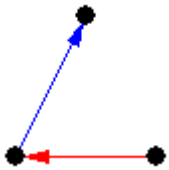	0.69961%	0.68499%	1.1034e-005	13.251	0
36	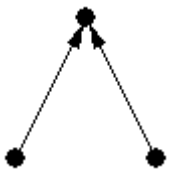	0.37547%	0.36762%	5.922e-006	13.251	0
12	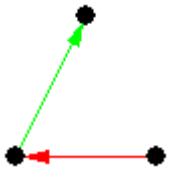	22.461%	22.005%	0.00036011	12.663	0

_ID	Adj	Frequency [Original]	Mean-Freq [Random]	Standard-Dev [Random]	Z-Score	p-Value
38	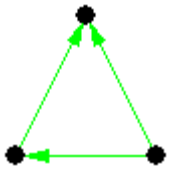	3.4218%	2.4727%	0.00075294	12.605	0
46	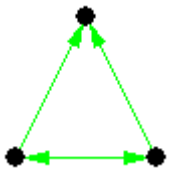	0.32854%	0.20012%	0.00010702	11.999	0
6	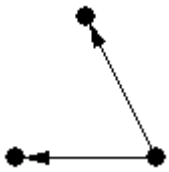	1.5254%	1.4933%	3.2321e-005	9.9311	0
166	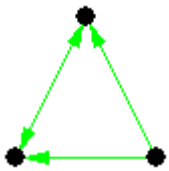	0.13053%	0.10225%	5.3625e-005	5.2752	0
36	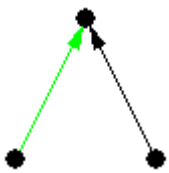	2.6826%	2.6228%	0.00012329	4.8492	0
38	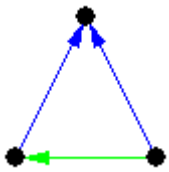	0.014667%	0.0055349%	2.378e-005	3.8403	0

Supplementary Figure S4: Size3 Network Motifs list obtained using FANMOD software. Sub-graphs are sorted based on Z-Score>2 (P-Value < 0.05). Each edge color specifies one special type of regulatory interaction between the two terms as follows below:

1) **miR-gene;** 2) **TF-gene** 3) **miR-TF** 4) **TF-miR**

Supplementary Table S1. Gene expression related to the effect of SARS-CoV-2 on A549 and NHBE cell lines. Log2FoldChange column shows the fold expression change of infected cells vs control (logarithmic scale base is 2) (*P*-values are calculated by the Wald t-test)

A549 cell line			NHBE cell line		
Gene-Name	**log2-FoldChange**	***P*-value**	**Gene-name**	**log2-FoldChange**	***P*-value**
CBSL	-1.570768605	0.033887755	**IFITM10**	-1.333473291	7.14E-11
ADCY5	-1.538884529	0.011786812	**MYLK**	-1.191256114	2.08E-08
PVRIG2P	-1.268185187	0.000652138	**CXCL14**	-1.174521485	1.41E-07
HRAT92	-1.255337642	0.003489927	**MAP7D2**	-1.129638152	4.85E-07
CILP2	-1.231141746	0.029523367	**STON1**	-1.100809904	1.43E-05
KRT4	-1.2253106	6.74E-07	**NANOS1**	-1.09955349	1.65E-05
RNF224	-1.214726256	0.042210693	**NID1**	-1.012415505	3.37E-06
LOC100289230	-1.185589577	0.047992834	**RBM20**	-1.000729651	0.000282974
SNAI3	-1.183406369	0.030288765	**VTCN1**	-0.960343372	4.28E-08
NECAB2	-1.118957783	0.000201977	**ATG9B**	-0.950922681	6.42E-06
COL20A1	-1.114510401	0.023853618	**METTL7A**	-0.947713376	2.86E-09
DGCR9	-1.07423789	0.004327137	**ZNF488**	-0.925232744	3.56E-05
SERTAD4	-0.991916082	0.007156344	**THBD**	-0.916581026	1.53E-10
GGN	-0.989736872	0.018541879	**PPARGC1A**	-0.912489135	1.24E-06
NUPR1	-0.986182604	3.63E-05	**OLFML2A**	-0.910277669	5.65E-14
ZNF575	-0.969425867	0.027450769	**KRT15**	-0.888978277	2.77E-13
PRRT3	-0.96232545	0.002396458	**ANKAR**	-0.86429133	0.002614627
LOC101928120	-0.953904793	0.025378402	**PDK4**	-0.855396413	0.002194278
LOC100129534	-0.945420436	0.011507521	**MXRA5**	-0.855393695	3.41E-11
ZGLP1	-0.938758831	0.02817289	**CYP4F3**	-0.841231556	0.000337333
BEX2	-0.904196833	0.042339532	**PRODH**	-0.833583401	0.002506262
LOC102723566	-0.85148517	0.047179714	**SEPP1**	-0.826207789	1.65E-07
UAP1L1	-0.844372666	1.81E-06	**POU2AF1**	-0.815631846	0.003036982

Supplementary Table S2. Transcription factors regulating shared DEGs between the A549 and NHBE cells treated with SARS-CoV-2. Titles of columns show the name of the databases used to extract TFs enriched for genes of A549 and NHBE cell lines. (They are selected based on *P*-value<0.05)

ARCHS4	ChEA	ENCODE	TRRUST	Enrichr, TF gene co-ocurrance
ETV7	RELA	STAT2	ARID3A	BATF2
BATF2	SOX2	STAT1	ATF4	ETV7
STAT2	IRF1	STAT1	BRCA1	IRF1
ZNFX1	IRF8	IRF1	CEBPD	STAT2
STAT1	FOXM1	RAD21	CIITA	ZNFX1
NFKB1	TCF21	E2F4	CREB5	IRF7
IRF7	SMAD2	FOXM1	EGR1	IRF9
IFI16	SMAD3	ZNF263	EGR2	PLEKHA4
PARP12	FOXA1	STAT3	FOXO1	ZC3HAV1
TRAFD1	FOXA1	CTCF	HDAC1	IFI16
ETV3L	CDX2	IKZF1	HIF1A	PARP12
BATF	MAF	CEBPB	HIVEP2	SP110
SP110	EGR1	FOS	HMGA1	STAT1
STAT3	SPI1	EP300	IRF1	ZBP1
ZFYVE26	PPAR	TBP	JUN	HES4
ZNF267	GATA4	TFAP2C	JUND	SP100
MTF1	BACH1	EP300	KLF4	TRAFD1

Supplementary Table S3. miRNAs extracted from the enrichment of shared DEGs of two cell lines (A549 and NHBE) treated with SARS-CoV-2 in public databases (They are selected based on *P*-value<0.05)

miRTarBase	TargetScan	mirDB	miRWalk
hsa-let-7	hsa-miR-1278	hsa-miR-543	hsa-miR-4803
hsa-let-7f-1	hsa-miR-1292	hsa-miR-4517	hsa-let-7a-3p
hsa-miR-1229	hsa-miR-151	hsa-miR-300	hsa-miR-5580-3p
hsa-miR-124	hsa-miR-1911	hsa-miR-302a-3p	hsa-miR-6506-3p
hsa-miR-1270	hsa-miR-208	hsa-miR-302b-3p	hsa-miR-656-3p
hsa-miR-1295	hsa-miR-21	hsa-miR-302c-3p	hsa-let-7f-1-3p
hsa-miR-130	hsa-miR-3117	hsa-miR-302d-3p	hsa-miR-6797-3p
hsa-miR-132	hsa-miR-3135	hsa-miR-372-3p	hsa-miR-7849-3p
hsa-miR-1	hsa-miR-3146	hsa-miR-373-3p	hsa-miR-98-3p
hsa-miR-144	hsa-miR-323b	hsa-miR-381-3p	hsa-miR-300
hsa-miR-1468	hsa-miR-3613	hsa-miR-520a-3p	hsa-miR-4760-5p
hsa-miR-146	hsa-miR-3622	hsa-miR-520b	hsa-miR-381-3p
hsa-miR-148	hsa-miR-3677	hsa-miR-520c-3p	hsa-miR-4757-3p
hsa-miR-155	hsa-miR-3681	hsa-miR-520d-3p	hsa-miR-548av-5p
hsa-miR-1587	hsa-miR-3684	hsa-miR-520e	hsa-miR-8061
hsa-miR-16-1	hsa-miR-4317	hsa-miR-4666a-5p	hsa-miR-7852-3p
hsa-miR-16-2	hsa-miR-4423	hsa-miR-493-5p	hsa-let-7b-3p

Supplementary Table S4. miRNAs extracted from the enrichment of TFs regulating DEG genes of two cell lines (A549 and NHBE) treated with SARS-CoV-2 in two miR database (miRTarBase &TargetScan) (They are selected based on *P*-value<0.05)

miRTarBase	TargetScan	selected microRNAs	TranscriptionFactors
hsa-let-7a-2	hsa-miR-1278	let-7a-2	HMGB2
hsa-let-7a	hsa-miR-1284	let-7a-2	SMARCA5
hsa-let-7b	hsa-miR-1296	let-7a	SMAD2
hsa-let-7c	hsa-miR-28	let-7a	HMGB2
hsa-let-7c	hsa-miR-2909	let-7b	SMAD2
hsa-let-7f-1	hsa-miR-3117	let-7b	HMGB2
hsa-let-7g	hsa-miR-3144	let-7c	SMARCA5
hsa-let-7g	hsa-miR-3177	let-7c	FOXO1
hsa-miR-106b	hsa-miR-3178	let-7c	CEBPB
hsa-miR-106b	hsa-miR-3200	let-7c	MYC
hsa-miR-107	hsa-miR-323b	let-7c	STAT2
hsa-miR-1183	hsa-miR-3545	let-7c	CREM
hsa-miR-1228	hsa-miR-3618	let-7c	CHD1
hsa-miR-1251	hsa-miR-3659	let-7f-1	SMAD2
hsa-miR-125a	hsa-miR-3682	let-7f-1	HMGB2
hsa-miR-1299	hsa-miR-3687	let-7g	HMGB2
hsa-miR-130b	hsa-miR-3935	let-7g	SMARCA5
hsa-miR-130b	hsa-miR-4280	let-7g	SMAD2

Supplementary Table S5. Transcription factors regulating miRNAs suppressing the shared DEG genes between A549 and NHBE cells treated with SARS-CoV-2. They were enriched in TRANSMIR database (They are selected based on *P*-value<0.05)

Transcription Factors	microRNAs
AR	let-7a
CDKN2A	miR-410
CEBPA	miR-26a
CREB1	miR-148a
DNMT1	miR-148a
DNMT3A	let-7b
E2F1	let-7a
E2F1	miR-16-2
E2F1	miR-195
E2F3	let-7a
E2F3	miR-195
E2F3	miR-26a
E2F7	miR-26a
EGR1	miR-148a
EGR3	miR-195
EHF	let-7b
EHMT2	let-7b

Supplementary Table S6. The following four regulatory types of relationships were used to construct the regulatory network in Cytoscape software

1- (miRNA → gene)		2- (TF → gene)		3- (miRNA → TF)		4- (TF → miRNA)	
microRNAS	**Genes**	**Transcription factrors**	**Genes**	**microRNAs**	**Transcription factors**	**Transcription factors**	**microRNAs**
miR-656	FBXW7	STAT2	IFITM3	let-7a-2	HMGB2	AR	let-7a
miR-656	CXCL5	STAT2	IFITM1	let-7a-2	SMARCA5	CDKN2A	miR-410
miR-656	AASDHPPT	STAT2	SAMD9L	let-7a	SMAD2	CEBPA	miR-26a
miR-656	EREG	STAT2	IFITM2	let-7a	HMGB2	CREB1	miR-148a
miR-98	WEE1	STAT2	UBE2L6	let-7b	SMAD2	DNMT1	miR-148a
miR-98	NCOA7	STAT2	IFI35	let-7b	HMGB2	DNMT3A	let-7b
miR-98	AASDHPPT	STAT2	SAMHD1	let-7c	SMARCA5	E2F1	let-7a
let-7a	WEE1	STAT2	IFIH1	let-7c	FOXO1	E2F1	miR-16-2
let-7a	NCOA7	STAT2	NAMPT	let-7c	CEBPB	E2F1	miR-195
let-7a	AASDHPPT	STAT2	TRIM25	let-7c	MYC	E2F3	let-7a
let-7b	WEE1	STAT2	TRIM21	let-7c	STAT2	E2F3	miR-195
let-7b	NCOA7	STAT2	HERC6	let-7c	CREM	E2F3	miR-26a
let-7b	AASDHPPT	STAT2	DTX3L	let-7c	CHD1	E2F7	miR-26a
let-7f-1	WEE1	STAT2	DDX58	let-7f-1	SMAD2	EGR1	miR-148a
let-7f-1	NCOA7	STAT2	STAT1	let-7f-1	HMGB2	EGR3	miR-195
let-7f-1	AASDHPPT	STAT2	ISG15	let-7g	HMGB2	EHF	let-7b
miR-5011	ERRFI1	STAT2	PARP14	let-7g	SMARCA5	EHMT2	let-7b
miR-5011	BTG3	STAT2	PARP9	let-7g	SMAD2	EIF2C2	let-7a
miR-5011	WEE1	STAT2	PARP12	let-7g	MYC	EIF2C2	let-7b
miR-5011	MBNL2	STAT2	PLSCR1	let-7g	STAT2	ELK1	miR-144

Supplementary Table S7. Biological Process Enrichment Results using the STRING WEB Tool

#term ID	Biological Process	Observed gene count	Background gene count	False discovery rate	Matching proteins in network (labels)
GO:0034097	Response to cytokine	45	1035	2.79E-25	ADAR,ANXA1,BIRC3,CEBPB,CXCL1,CXCL2,ETS1,FOSL1,FOXO1,GBP1,HIF1A,IFI35,IFITM1,IFITM2,IFITM3,IL6,IRF1,IRF7,IRF9,ISG15,MAP3K8,MYC,NFIL3,NFKB1,NFKB2,NFKBIA,NFYB,OAS1,OAS2,OAS3,PLSCR1,PSME2,PTGS2,RELB,RNF138,SAMHD1,SMAD3,SMARCA5,SOX2,SP100,STAT1,STAT2,STAT5A,TRIM21,TRIM25
GO:0006952	Defense response	46	1234	1.24E-23	ADAR,ANXA1,ANXA3,BATF2,C1S,C3,CEBPB,CFB,CXCL1,CXCL2,DDX58,DTX3L,FOSL1,GBP1,HIF1A,HMGB2,IFI16,IFI35,IFIH1,IFITM1,IFITM2,IFITM3,IL6,IRF1,IRF7,IRF9,ISG15,NFKB1,NFKB2,OAS1,OAS2,OAS3,PARP14,PARP9,PLSCR1,PTGS2,RELB,SAMHD1,SP100,STAT1,STAT2,TNFAIP3,TRIM14,TRIM21,TRIM25,ZC3HAV1
GO:0051707	Response to other organism	40	835	1.24E-23	ADAR,ANXA3,BATF2,C3,CEBPB,CXCL1,CXCL2,DDX58,DTX3L,FOSL1,GBP1,HERC6,HMGB2,IFI16,IFI44,IFIH1,IFITM1,IFITM2,IFITM3,IL6,IRF1,IRF7,IRF9,ISG15,NFKB1,NFKB2,NFKBIA,OAS1,OAS2,OAS3,PARP9,PLSCR1,PTGS2,SAMHD1,SMAD3,STAT1,STAT2,TNFAIP3,TRIM25,ZC3HAV1
GO:0051607	Defense response to virus	24	181	7.77E-23	ADAR,DDX58,DTX3L,GBP1,IFI16,IFIH1,IFITM1,IFITM2,IFITM3,IL6,IRF1,IRF7,IRF9,ISG15,OAS1,OAS2,OAS3,PARP9,PLSCR1,SAMHD1,STAT1,STAT2,TRIM25,ZC3HAV1
GO:0071345	Cellular response to cytokine stimulus	40	953	4.11E-22	ADAR,ANXA1,BIRC3,CEBPB,CXCL1,CXCL2,FOXO1,GBP1,HIF1A,IFI35,IFITM1,IFITM2,IFITM3,IL6,IRF1,IRF7,IRF9,ISG15,MAP3K8,MYC,NFIL3,NFKB1,NFKBIA,NFYB,OAS1,OAS2,OAS3,PSME2,PTGS2,RNF138,SAMHD1,SMAD3,SMARCA5,SOX2,SP100,STAT1,STAT2,STAT5A,TRIM21,TRIM25
GO:0006950	Response to stress	65	3267	8.68E-22	ADAR,ANXA1,ANXA3,BATF2,C1S,C3,CDK1,CEBPB,CFB,CXCL1,CXCL2,DDX58,DTX3L,ETS1,FANCI,FOSL1,FOXO1,GBP1,HIF1A,HMGB2,IFI16,IFI35,IFIH1,IFITM1,IFITM2,IFITM3,IL6,IRF1,IRF7,IRF9,ISG15,MAFF,MAP3K8,MYC,NFKB1,NFKB2,NFKBIA,OAS1,OAS2,OAS3,PARP14,PARP9,PLSCR1,PPP1R15A,PROS1,PTGS2,RELB,RNF138,SAMHD1,SMAD2,SMAD3,SMC3,SOX2,SP100,STAT1,STAT2,TNFAIP3,TOP2A,TRIM14,TRIM21,TRIM25,TSC22D3,UBE2L6,UPP1,ZC3HAV1
GO:0009615	Response to virus	26	270	8.68E-22	ADAR,DDX58,DTX3L,FOSL1,GBP1,IFI16,IFI44,IFIH1,IFITM1,IFITM2,IFITM3,IL6,IRF1,IRF7,IRF9,ISG15,OAS1,OAS2,OAS3,PARP9,PLSCR1,SAMHD1,STAT1,STAT2,TRIM25,ZC3HAV1

Supplementary Table S8. Molecular Function Enrichment Results using the STRING WEB Tool

#Term ID	Molecular functions	Observed gene count	Background gene count	False discovery rate	Matching proteins in your network (labels)
GO:0003677	DNA binding	51	2457	3.82E-16	ADAR,ANXA1,BATF2,CASP8AP2,CEBPB,CHD1,CREM,DDX58,DEK,ETS1,FANCI,FOSL1,FOXO1,HELZ2,HIF1A,HIVEP2,HMGB2,IFI16,IFIH1,IRF1,IRF7,IRF9,MAF,MAFF,MXI1,MYC,NFIL3,NFKB1,NFKB2,NFYB,PLSCR1,RELB,RNF138,SMAD2,SMAD3,SMARCA5,SMC2,SOX2,SP100,SP110,STAT1,STAT2,STAT5A,SUZ12,TIPARP,TNFAIP3,TOP2A,TRIM21,WDHD1,ZBED2,ZNF146
GO:0003676	Nucleic acid binding	56	3332	1.98E-14	ADAR,ANXA1,BATF2,CASP8AP2,CEBPB,CHD1,CREM,DDX58,DEK,ETS1,FANCI,FOSL1,FOXO1,HELZ2,HIF1A,HIVEP2,HMGB2,IFI16,IFIH1,IRF1,IRF7,IRF9,MAF,MAFF,MXI1,MYC,NFIL3,NFKB1,NFKB2,NFYB,OAS1,OAS2,OAS3,PLSCR1,RELB,RNF138,SAMHD1,SMAD2,SMAD3,SMARCA5,SMC2,SOX2,SP100,SP110,STAT1,STAT2,STAT5A,SUZ12,TIPARP,TNFAIP3,TOP2A,TRIM21,WDHD1,ZBED2,ZCCHC10,ZNF146
GO:0140110	Transcription regulator activity	42	2069	1.40E-12	BATF2,CASP8AP2,CEBPB,CREM,ETS1,FOSL1,FOXO1,HELZ2,HIF1A,HIVEP2,HMGB2,IFI16,IRF1,IRF7,IRF9,MAF,MAFF,MXI1,MYC,NCOA7,NFIL3,NFKB1,NFKB2,NFYB,PARP9,PLSCR1,RELB,SMAD2,SMAD3,SMARCA5,SOX2,SP100,SP110,STAT1,STAT2,STAT5A,TRIM25,TSC22D3,WDHD1,ZBED2,ZNF146,ZNFX1
GO:0003700	DNA-binding transcription factor activity	38	1749	4.08E-12	BATF2,CEBPB,CREM,ETS1,FOSL1,FOXO1,HIF1A,HIVEP2,HMGB2,IFI16,IRF1,IRF7,IRF9,MAF,MAFF,MXI1,MYC,NFIL3,NFKB1,NFKB2,NFYB,PLSCR1,RELB,SMAD2,SMAD3,SMARCA5,SOX2,SP100,SP110,STAT1,STAT2,STAT5A,TRIM25,TSC22D3,WDHD1,ZBED2,ZNF146,ZNFX1

Supplementary Table S9. Cellular Component Enrichment Results using the STRING WEB Tool

#term ID	Cellular Component	Observed gene count	Background gene count	False discovery rate	matching proteins in your network (labels)
GO:0005634	Nucleus	77	6892	3.60E-12	ADAR,ANXA1,BATF2,BIRC3,CASP8AP2,CDK1,CEBPB,CHD1,CREM,DEK,DEPDC1,DLGAP5,DTX3L,ETS1,FANCI,FOSL1,FOXO1,HELZ2,HERC6,HIF1A,HIVEP2,HMGB2,IFI16,IFI35,IFIH1,IRF1,IRF7,IRF9,ISG15,LAP3,MAF,MAFF,MXI1,MYC,NAMPT,NCOA7,NFIL3,NFKB1,NFKB2,NFKBIA,NFYB,OAS1,OAS2,OAS3,PARP12,PARP14,PARP9,PLSCR1,PSME1,PSME2,RELB,SAMHD1,SMAD2,SMAD3,SMARCA5,SMC2,SMC3,SOX2,SP100,SP110,STAT1,STAT2,STAT5A,SUZ12,TIPARP,TNFAIP3,TOP2A,TRIM21,TRIM25,TSC22D3,UBE2L6,UPP1,WDHD1,WEE1,ZC3HAV1,ZNF146,ZNFX1
GO:0005654	Nucleoplasm	54	3446	3.60E-12	ADAR,ANXA1,BIRC3,CASP8AP2,CDK1,CEBPB,CHD1,DEK,DTX3L,ETS1,FANCI,FOSL1,FOXO1,HELZ2,HIF1A,HIVEP2,HMGB2,IFI16,IRF1,IRF7,IRF9,ISG15,LAP3,MAFF,MYC,NAMPT,NFKB1,NFKB2,NFYB,OAS2,OAS3,PARP9,PSME1,PSME2,RELB,SAMHD1,SMAD2,SMAD3,SMARCA5,SMC2,SMC3,SOX2,SP100,STAT1,STAT2,STAT5A,SUZ12,TOP2A,TRIM21,TRIM25,UBE2L6,UPP1,WDHD1,WEE1
GO:0031981	Nuclear lumen	57	4030	1.11E-11	ADAR,ANXA1,BIRC3,CASP8AP2,CDK1,CEBPB,CHD1,DEK,DTX3L,ETS1,FANCI,FOSL1,FOXO1,HELZ2,HIF1A,HIVEP2,HMGB2,IFI16,IRF1,IRF7,IRF9,ISG15,LAP3,MAFF,MXI1,MYC,NAMPT,NFKB1,NFKB2,NFYB,OAS2,OAS3,PARP9,PLSCR1,PSME1,PSME2,RELB,SAMHD1,SMAD2,SMAD3,SMARCA5,SMC2,SMC3,SOX2,SP100,STAT1,STAT2,STAT5A,SUZ12,TOP2A,TRIM21,TRIM25,UBE2L6,UPP1,WDHD1,WEE1,ZNF146
GO:0070013	Intracellular organelle lumen	62	5162	3.93E-10	ADAR,ANXA1,BIRC3,C3,CASP8AP2,CDK1,CEBPB,CHD1,CXCL1,DEK,DTX3L,ETS1,FANCI,FOSL1,FOXO1,HELZ2,HIF1A,HIVEP2,HMGB2,IFI16,IL6,IRF1,IRF7,IRF9,ISG15,LAP3,MAFF,MXI1,MYC,NAMPT,NFKB1,NFKB2,NFYB,OAS2,OAS3,PARP9,PLSCR1,PROS1,PSME1,PSME2,PTGS2,RELB,SAMHD1,SMAD2,SMAD3,SMARCA5,SMC2,SMC3,SOX2,SP100,STAT1,STAT2,STAT5A,SUZ12,TOP2A,TRIM21,TRIM25,UBE2L6,UPP1,WDHD1,WEE1,ZNF146
GO:0005829	Cytosol	57	4958	2.63E-08	ANXA1,ANXA3,BIRC3,CDK1,CKAP2,DDX58,DEPDC1B,DLGAP5,DTX3L,FANCI,FOSL1,FOXO1,GBP1,HERC6,HIF1A,IFI16,IFI35,IFIH1,IRF1,IRF7,IRF9,ISG15,LAP3,MAP3K8,MXI1,NAMPT,NFKB1,NFKB2,NFKBIA,OAS1,OAS2,OAS3,PARP14,PARP9,PLSCR1,PPP1R15A,PSME1,PSME2,RELB,SASS6,SERPINB8,SMAD2,SMAD3,SMC2,SMC3,SOX2,STAT1,STAT2,STAT5A,TNFAIP3,TRIM21,TRIM25,TSC22D3,UBE2L6,UPP1,ZC3HAV1,ZNF146

Supplementary Table S10. Biochemical pathway enrichment results (kegg) using the string web tool

#term ID	Term description (KEGG pathway)	Observed gene count	Background gene count	False discovery rate	Matching proteins in network (labels)
hsa04621	NOD-like receptor signaling pathway	17	166	2.08E-14	BIRC3,CXCL1,CXCL2,GBP1,IFI16,IL6,IRF7,IRF9,NAMPT,NFKB1,NFKBIA,OAS1,OAS2,OAS3,STAT1,STAT2,TNFAIP3
hsa05162	Measles	15	133	1.91E-13	ADAR,DDX58,IFIH1,IL6,IRF7,IRF9,NFKB1,NFKBIA,OAS1,OAS2,OAS3,STAT1,STAT2,STAT5A,TNFAIP3
hsa05168	Herpes simplex infection	15	181	8.39E-12	C3,CDK1,DDX58,IFIH1,IL6,IRF7,IRF9,NFKB1,NFKBIA,OAS1,OAS2,OAS3,SP100,STAT1,STAT2
hsa05164	Influenza A	14	168	3.94E-11	ADAR,DDX58,IFIH1,IL6,IRF7,IRF9,NFKB1,NFKBIA,OAS1,OAS2,OAS3,STAT1,STAT2,TRIM25
hsa05167	Kaposi's sarcoma-associated herpesvirus infection	13	183	1.38E-09	C3,CXCL1,CXCL2,HIF1A,IL6,IRF7,IRF9,MYC,NFKB1,NFKBIA,PTGS2,STAT1,STAT2
hsa04064	NF-kappa B signaling pathway	10	93	5.14E-09	BIRC3,CXCL2,DDX58,NFKB1,NFKB2,NFKBIA,PTGS2,RELB,TNFAIP3,TRIM25
hsa05160	Hepatitis C	11	131	6.20E-09	DDX58,IRF1,IRF7,IRF9,NFKB1,NFKBIA,OAS1,OAS2,OAS3,STAT1,STAT2
hsa05161	Hepatitis B	11	142	1.21E-08	DDX58,IFIH1,IL6,IRF7,MYC,NFKB1,NFKBIA,SMAD3,STAT1,STAT2,STAT5A
hsa04668	TNF signaling pathway	10	108	1.32E-08	BIRC3,CEBPB,CXCL1,CXCL2,IL6,MAP3K8,NFKB1,NFKBIA,PTGS2,TNFAIP3
hsa05166	HTLV-I infection	13	250	2.59E-08	CREM,ETS1,FOSL1,IL6,MYC,NFKB1,NFKB2,NFKBIA,NFYB,RELB,SMAD2,SMAD3,STAT5A
hsa04657	IL-17 signaling pathway	9	92	5.00E-08	CEBPB,CXCL1,CXCL2,FOSL1,IL6,NFKB1,NFKBIA,PTGS2,TNFAIP3
hsa05134	Legionellosis	7	54	4.45E-07	C3,CXCL1,CXCL2,IL6,NFKB1,NFKB2,NFKBIA